Neutron Resonance Parameters of the Erbium Isotopes*

S. F. MUGHABGHAB, R. E. CHRIEN, AND M. R. BHAT
Brookhaven National Laboratory, Upton, New York
(Received 14 June 1967)

Neutron resonance parameters, s-wave strength functions, level densities, and radius parameters for Er^{162}, Er^{164}, Er^{166}, Er^{167}, and Er^{168} have been determined from total neutron cross-section measurements. Average cross-section measurements for Er^{162}, Er^{164}, and Er^{167} have been analyzed to determine neutron strength functions in the keV region, and the results are compared to those derived from the low-energy resonance-parameter data. A spin cutoff factor σ of 2.5 ± 0.8 is derived from a comparison of the level densities of Er^{162}, Er^{164}, and Er^{167}. The thermal-neutron total cross sections were measured for Er^{168} and Er^{164}, and the paramagnetic scattering cross section for Er^{168} was determined to be 26.1 ± 2.5 b.

I. INTRODUCTION

THE s-wave neutron strength function has been the subject of considerable theoretical and experimental investigations because of its importance in the development of the optical model. Early calculations by Feshbach, Porter, and Weisskopf[1] (FPW) showed clearly that the "cloudy crystal ball" model fitted the general trend of the experimental values of the strength function better than the "black nucleus" model. With the improvement in experimental techniques, the more accurate data on strength functions, especially in the region around mass number $A=160$, made it clear that the FPW optical-model calculations do not adequately describe the experimental values in this region. The inclusion of deformation[2] in the optical model led to a splitting of the 4-S giant resonance peak in the strength function into two peaks located around $A=140$ and 180. More recently, Feshbach, Shakin, and Lemmer[3] introduced the so-called intermediate model to take into account the effect of the two-particle–one-hole states, also known as the doorway states, on quantities such as total cross sections and strength functions. Their theory predicts that one would observe fluctuations in the strength function as a function of energy and mass number A. The latter type of fluctuation is superimposed on the giant single-particle resonance behavior.

For the past three years, we have been devoting our efforts to the study of neutron-transmission measurements in the rare-earth region on highly enriched isotopes of Gd, Dy, Yb, and Er. The primary purpose of these investigations is to determine the systematic behavior of the strength function with atomic mass number. As a byproduct of these studies, we obtained the following quantities for the various isotopes: (a) resonance parameters, (b) potential scattering radii, (c) thermal cross sections, and (d) level densities. Summaries on strength functions[4] and on the systematic properties of neutron resonances in the rare-earth region[5] have been reported in previous publications. In this paper, we discuss in detail our results on the Er isotopes. Preliminary results on the Er isotopes have been reported.[6,7] A survey of the literature at the start of this experiment revealed that very few measurements were made on the separated isotopes. Møller *et al.*,[8] using the BNL crystal spectrometer, studied the two low-lying resonances in Er^{167} at 0.460 and 0.584 eV. Later, Vertebny *et al.*,[9] reported some measurements on the separated Er isotopes in a narrow energy region. Early unpublished BNL fast-chopper data, General Atomic data on the linac, and recent preliminary Columbia results on the separated isotopes can be found in Goldberg *et al.*[10]

II. EXPERIMENTAL PROCEDURE

Neutron-transmission measurements were carried out on enriched Er isotopes, using the fast-chopper facility at the Brookhaven Graphite Research Reactor (BGRR). The samples in the form of powdered oxides were obtained on loan from Oak Ridge National Laboratory. The powdered samples were carefully packed in steel and plastic holders to ensure uniform thickness. The enrichment and impurities of the various samples are shown in Table I. Also listed are the sample thicknesses calculated using the stoichiometric formula Er_2O_3.

In order to span the neutron energy range from thermal to a few keV, generally five separate runs for each isotope were carried out. For neutron energies greater

* Work performed under the auspices of the U. S. Atomic Energy Commission.

[1] H. Feshbach, C. E. Porter, and V. F. Weisskopf, Phys. Rev. **96**, 448 (1954).

[2] D. M. Chase, L. Wilets, and A. R. Edmonds, Phys. Rev. **110**, 1080 (1958).

[3] H. Feshbach, A. K. Kerman, and R. H. Lemmer, Ann. Phys. (N. Y.) **41**, 230 (1967).

[4] R. E. Chrien and S. F. Mughabghab, in *Nuclear Structure Study with Neutrons*, edited by M. Nève de Mévergnies *et al.* (North-Holland Publishing Company, Amsterdam, 1966), p. 524.

[5] R. E. Chrien, S. F. Mughabghab, M. R. Bhat, and A. P. Jain, Phys. Letters **24B**, 573 (1967).

[6] S. F. Mughabghab, R. E. Chrien, and M. R. Bhat, Bull. Am. Phys. Soc. **11**, 334 (1966).

[7] S. F. Mughabghab, R. E. Chrien, and M. R. Bhat, Bull. Am. Phys. Soc. **12**, 105 (1967).

[8] H. B. Møller, F. J. Shore, and V. L. Sailor, Nucl. Sci. Eng. **8**, 183 (1960).

[9] V. P. Vertebny, M. F. Vlasov, A. L. Kiriljuk, V. V. Koloty, M. V. Pasechnik, and N. A. Trofimova, in *Nuclear Structure Study with Neutrons*, edited by M. Néve de Mévergnies *et al.* (North-Holland Publishing Company, Amsterdam, 1966), p. 572.

[10] M. D. Goldberg, S. F. Mughabghab, S. N. Purohit, B. A. Magurno, and V. M. May, *Brookhaven National Laboratory Report No. 325* (U. S. Government Printing Office, Washington, D. C., 1967), 2nd ed., Suppl. 2, Vol. IIC.

TABLE I. Isotopic composition and sample thickness of Er samples. Each column refers to a particular sample in terms of its main isotope. The rows give the percentage abundance of the indicated isotope, except that the last row gives the total sample thickness in atoms/barn.

% Isotopic compositions	Er^{162}	Er^{164}	Er^{166}	Er^{167}	Er^{168}
Er^{162}	20.4 ±0.1	0.09	<0.005	<0.01	<0.005
Er^{164}	3.91±0.05	62.7 ±0.1	<0.005	<0.05	<0.005
Er^{166}	33.5 ±0.1	20.6 ±0.1	99.97 ±0.01	3.50±0.05	<0.005
Er^{167}	17.6 ±0.1	7.87±0.1	0.03 ±0.01	91.1 ±0.1	0.013
Er^{168}	17.3 ±0.1	6.4 ±0.1	<0.01	4.89±0.05	99.99
Er^{170}	7.29±0.05	2.29±0.05	<0.005	0.47±0.05	<0.005
$n(10^{-3}$ atom/b)	9.93	10.58	10.93	9.26	14.44

than 0.712 eV, a flight path of 29.74 m and a bank of BF_3 detectors were used; the chopper was spun at speeds of 10 000, 6000, and 2000 rpm, with respective input delays of 0, 224, 512 μsec. The associated channel widths of the time-of-flight analyzer were 0.5, 1, and 4 μsec, respectively. The nominal time resolution was 50 nsec/m at 10 000 rpm. As we were approaching the scheduled date for the shutdown of the fast-chopper facility at the BGRR, we were able to carry out only two measurements in the thermal region on Er^{164} and Er^{168}. For these sets of measurements, spanning an energy region of 2.19–0.228 eV and 0.662–0.021 eV, a 10-m flight path and a He^3 detector were utilized; the chopper was run at a speed of 400 rpm. The channel widths were 2 and 8 μsec, respectively.

The raw data were accumulated and later stored on magnetic tapes in an on-line SDS-910 computer,[11] which is time-shared with a slow-chopper experiment. Since the cycling mechanism was located at the exit stator of the chopper and the samples were inserted in a slit package located at the entrance stator, a method was devised to handle the cycling procedure. For each transmission measurement, it was necessary to take two runs: one in which a sample and a dummy were placed, for example, in the east and west slits of the two-beam hole of the fast chopper, respectively; another in which sample and open were interchanged. The appropriate slit was selected by a moving stage carrying three 3-in. lucite plugs at the exit stator. The stage was programmed to repeat 20-min cycles in which the east slit was covered, then the west slit, and finally both were covered for a background measurement. The backgrounds per channel for the open beam and the sample spectra were generally determined by two methods: (a) by calculations from the total background counts, the elapsed times, and the chopper speed, (b) by the method of "blackout" resonances for runs where strong resonances were present. A typical background rate is about 10% of the open beam spectrum. The zero time of the high-energy run was deduced from the zero time of the γ-ray flash and from the position of the Na line at 2.85 keV.

[11] R. E. Chrien, S. Rankowitz, and R. J. Spinrad, Rev. Sci. Instr. 35, 1150 (1964).

III. ANALYSIS OF DATA

This section consists of two parts. The first part deals with the reduction of the raw data to obtain sample transmissions and the subsequent extraction of resonance parameters by the Breit-Wigner area analysis. The second part describes briefly the method of obtaining the strength functions from the energy variation of the transmission curve in the keV region.

A. Resonance Parameters

The initial steps of analysis, consisting in reducing the raw data to transmission form, are performed on the SDS–910 computer. These include the following: (a) smoothing the background, using a least-squares fitting procedure; (b) normalizing the open to sample running time; (c) subtracting the background counts from the open beam and sample spectra; (d) calculating a "cross slit" transmission by dividing the sample spectrum of *one* slit by the open spectrum from the *other* (it should be emphasized that this is not a true transmission because of spectrum differences between the two slits); and (e) finally, taking a geometric mean of the two cross slit transmissions to obtain the true transmission. The final transmission is punched on paper tape which thereafter is converted to punched cards by means of an IBM tape-to-card converter.

To extract resonance parameters from the transmission data, a modified version of the Atta-Harvey[12] code of Breit-Wigner area analysis written for the IBM-7094 computer is used. A detailed discussion of the modifications has been previously described.[13,14] Since no attempt has been made to obtain radiation widths, a weighted average value of 88±9 mV is assumed in the analysis for all resonances in all the isotopes. This is based on the BNL crystal spectrometer[8] and the General Atomic linac values of radiation widths.[10] For the even-odd Er^{167} isotope, a statistical weight factor of 0.5 is assumed.

[12] S. E. Atta and J. A. Harvey, Oak Ridge National Laboratory Report No. ORNL 3205, 1961 (unpublished).
[13] R. E. Chrien, Phys. Rev. 141, 1129 (1966).
[14] M. R. Bhat and R. E. Chrien, Phys. Rev. 155, 1362 (1967).

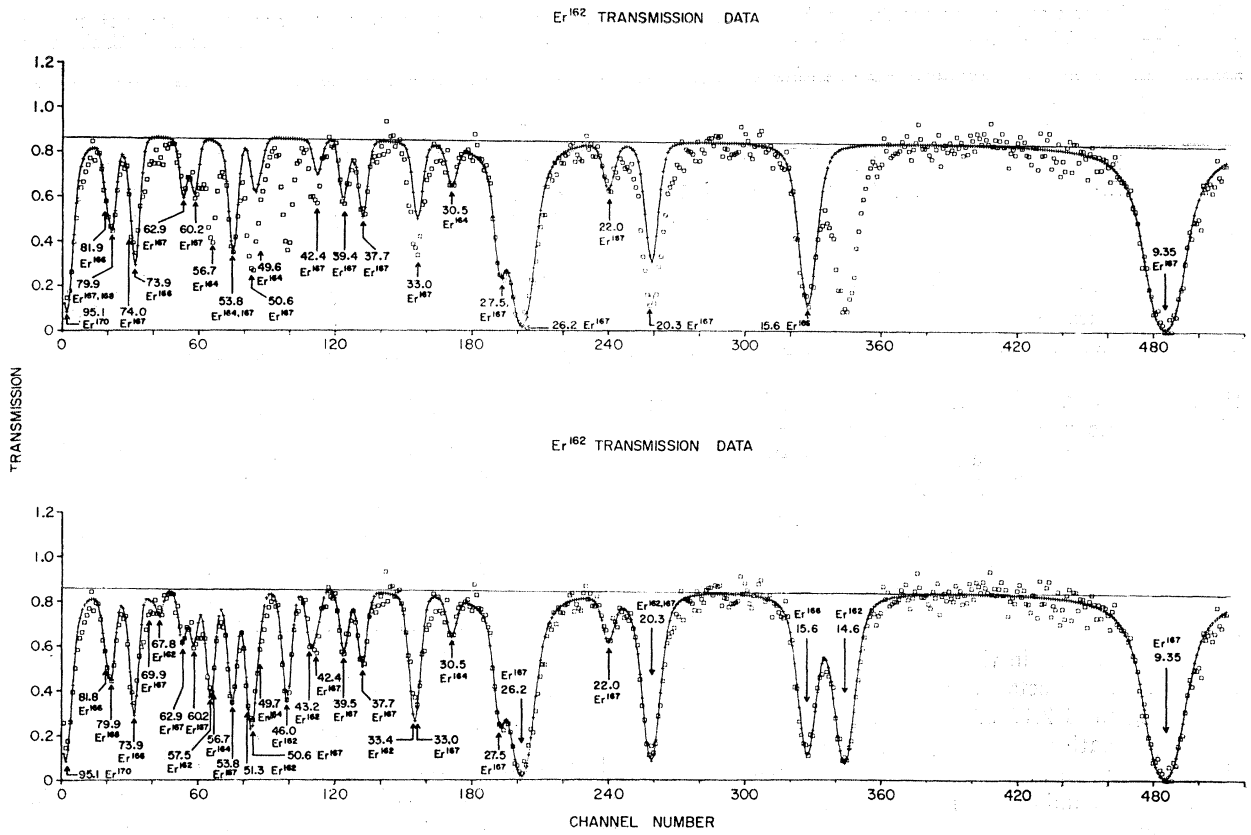

FIG. 1. The transmission of Er^{162} in the energy region 8.67–97.2 eV. The bottom figure shows the experimental data and the final theoretical fit. In the upper figure, the theoretical curve includes only the contributions of the potential scattering and of the isotopic impurity resonances.

Isotope identification of resonances appearing in highly enriched samples such as Er^{166}, Er^{167}, and Er^{168} is straightforward. However, the transmission of samples with poor enrichment, like Er^{162} and to a lesser extent Er^{164}, require special study. For these cases, a detailed knowledge of the resonance parameters of the isotopic impurities is necessary. Such a study is especially required when resonances belonging to different isotopes are located at nearly the same energy. Figure 1 illustrates the method for assigning resonances to Er^{162}. Some isolated resonances which appear only in this sample, like the 14.6-eV resonance, can readily be assigned to Er^{162}. However, a few of the Er^{162} resonance energies overlap with other Er resonances. An example of the latter is afforded by the 20-eV resonance in Er^{167}. For these types of resonances, it is difficult to ascertain by inspection the Er^{162} resonances. By including the contribution of all isotopic impurities to the transmission, it is possible to unfold the contribution due to Er^{162}. The solid-smooth curve in the upper part of Fig. 1 represents the transmission due to the impurities and is generated by a Calcomp plotter. Below each dip is designated the Er impurity responsible for the observed effect. Resonances can then be attributed to Er^{162} at dips where the deviation between the calculated curve and experimental points is appreciable. This type of analysis is extended up to an energy of 250 eV for Er^{162} and Er^{164}.

B. Strength Function Analysis

Averaging the Breit-Wigner total cross section relation for s-wave neutrons over an energy interval containing many resonances, one obtains[1]

$$\langle\sigma_T\rangle=4\pi(R')^2+2\pi^2\lambda^2\sqrt{E}\frac{\langle\Gamma_n^0\rangle}{D}+0\left(\frac{\langle\Gamma_n^0\rangle}{D}\right)^2, \quad (1)$$

where R' is the potential scattering radius, λ is the deBroglie wave length divided by 2π for the incident neutron whose energy is E, $\langle\Gamma_n^0\rangle$ is the average reduced neutron width, and D is the average level spacing. The contribution of the higher-order terms to the cross section is small and therefore has been neglected in the analysis. The ratio $\langle\Gamma_n^0\rangle/D$, the average reduced neutron width to average level spacing, is called the strength function. It should be noted that the second term has a $1/v$ dependence; hence, when $\langle\sigma_T\rangle$ is plotted against time of flight, one obtains a straight line whose slope is proportional to the strength function and whose intercept at zero time of flight is equal to the potential

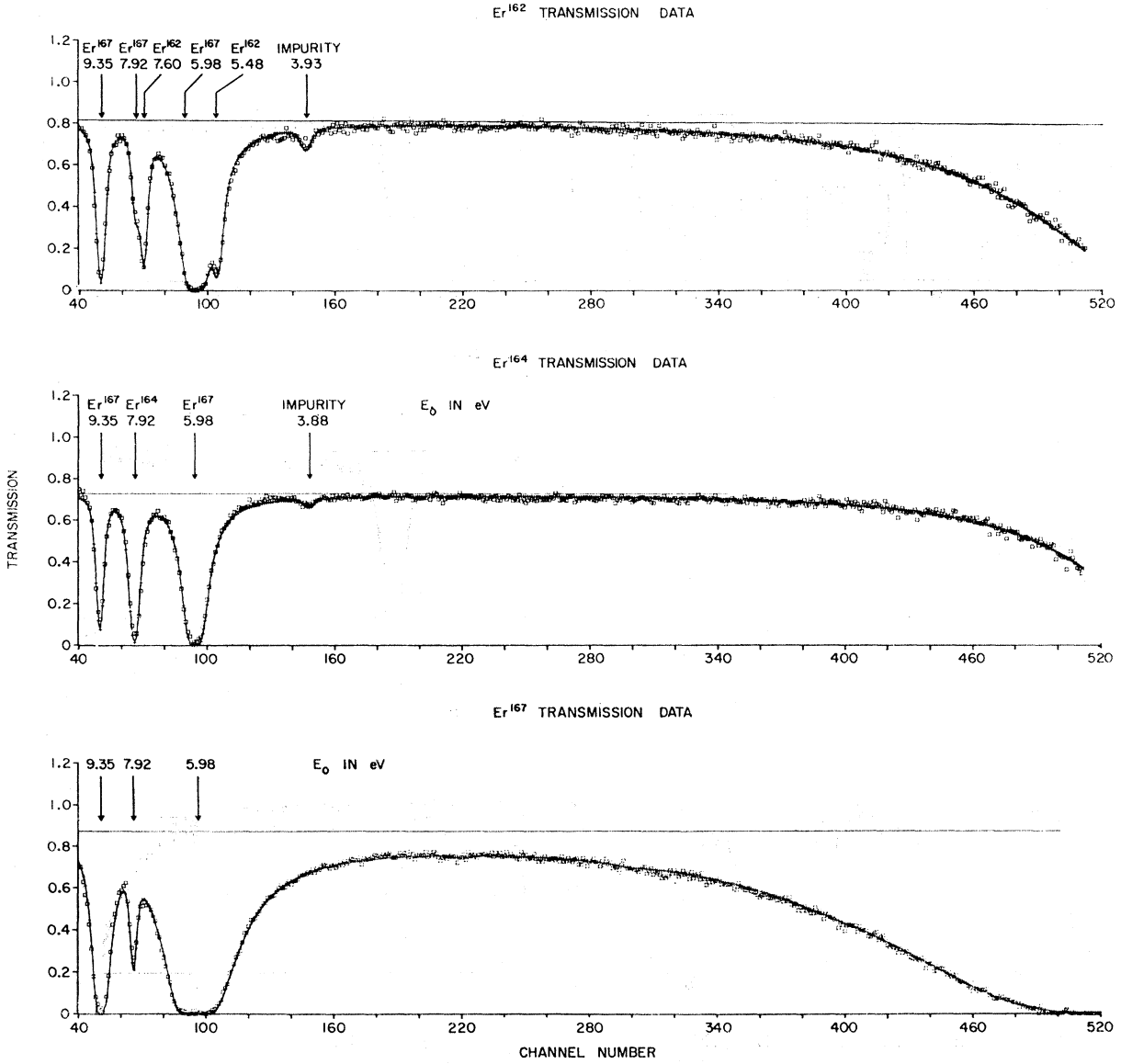

FIG. 2. The transmission of Er^{162}, Er^{164}, and Er^{167} in the energy range 10.6–0.712 eV. The contributions of the 0.460 and 0.584 eV resonances of Er^{167} have been included in the calculations.

scattering cross section. The strength-function values are derived by the use of a program which makes a least-squares fit to the average transmission after correcting for impurities, sample thickness effects, and level fluctuations.[13] Two conditions are imposed on the result in order for it to be considered acceptable: (a) The value of the strength function must converge rapidly after all corrections have been applied. For isotopes with small average level spacings, this criterion is readily satisfied because each energy interval contains several hundred resonances. (b) The value of nuclear scattering radius R' obtained from this analysis must agree within the experimental error with that derived from curve fitting in the low-energy region.

IV. RESULTS AND DISCUSSION

A. Resonance Parameters

Figure 2 represents our fitted data for Er^{162}, Er^{164}, and Er^{167} in the energy region 10.6–0.712 eV. The strong effect observed at the low-energy side of the transmission curve is due to the 0.460- and 0.584-eV resonances in Er^{167}. The parameters of these two resonances were obtained from two measurements in the thermal-energy region on an Er^{164} sample which contains 7.87% Er^{167} impurity. The parameters obtained from area analysis are fed into a code which computes the transmission, including instrumental resolution and Doppler broadening in the calculations. The shape of

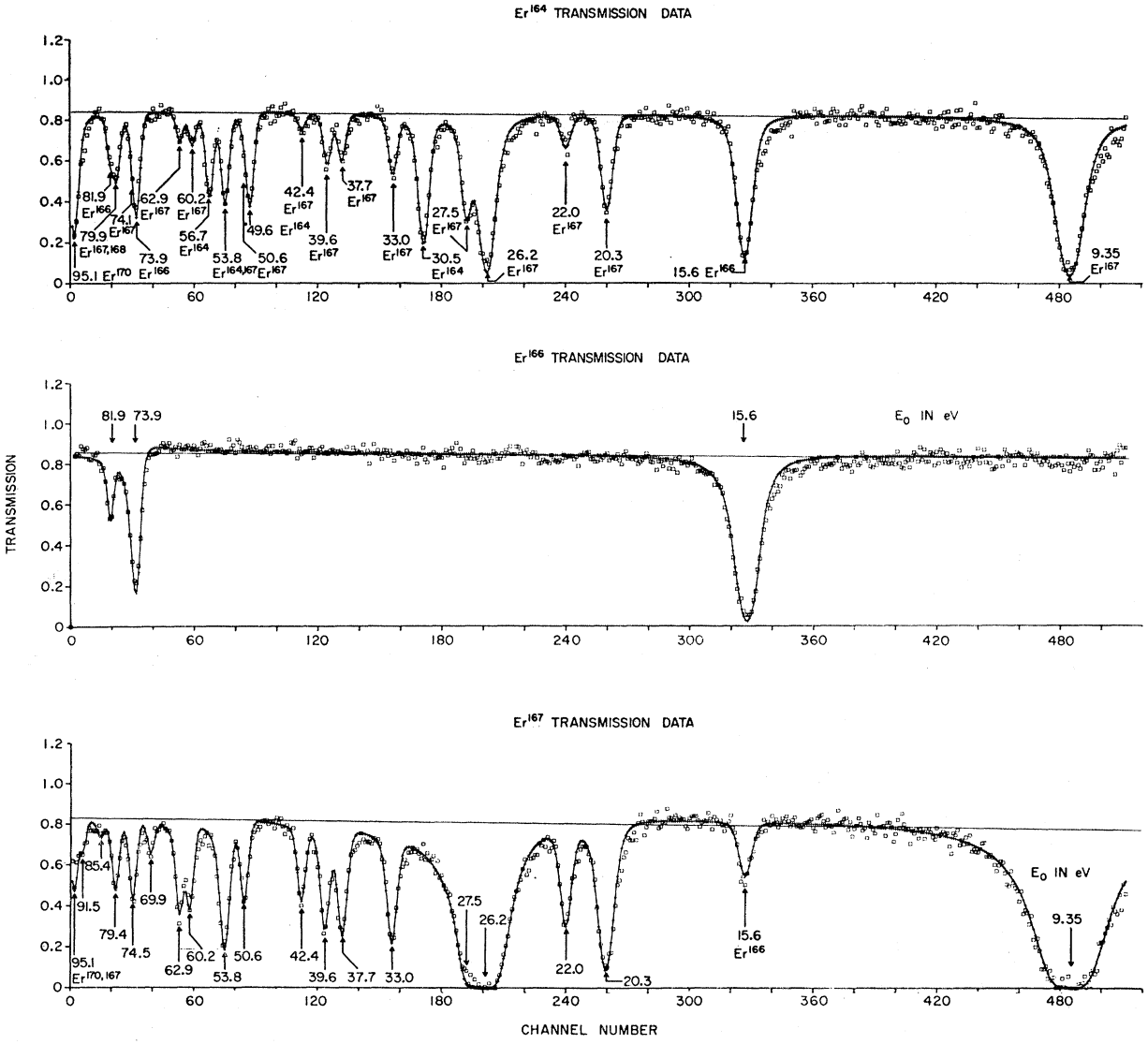

FIG. 3. The fitted transmission curves of Er^{164}, Er^{166}, and Er^{167} in the energy range 8.67–97.2 eV. Er^{166} does not have any positive energy resonances below 15.6 eV.

the instrumental resolution function is assumed to be Gaussian. It is interesting to note that both Er^{164} and Er^{167} have a resonance near 7.98 eV. The nature of the resonances near 3.9 eV appearing in the transmissions of Er^{162} and Er^{164} is not very well understood, but we believe that they are due to a Tm impurity. Thulium has a strong resonance at 3.90±0.02 eV.[15] From the measured $fg\Gamma_n^0$ values in the Er^{162} and Er^{164} samples (f is the fractional abundance of the isotope responsible for the observed dip), these resonances can be accounted for by thulium fractional abundances of 2.7×10^{-4} and 1.1×10^{-4} in Er^{162} and Er^{164}, respectively. The spectrographic analysis of Oak Ridge National Laboratory lists an upper limit for Tm impurity of $f<5.0\times10^{-4}$ for the Er isotopes.

In Fig. 3 and at the bottom of Fig. 1 we show the fitted transmission curves for Er^{164}, Er^{166}, Er^{167}, and Er^{162}, respectively, in the energy interval 97.2–8.67 eV. Recent self-indication measurements conducted at Columbia[16] indicate that the "level" at 26.2 eV in Er^{167} is resolved into two resonances of equal strengths and located at 26.03 and 26.64 eV. Transmission measurements were not able to resolve these resonances. In addition, we were unable to resolve the level at 62.9 eV in Er^{167} into its components at 62.19 and 62.86 eV.

[15] R. Al-Kital, G. Brunhart, S. S. Malik, J. P. Roberge, and V. L. Sailor, Nucl. Phys. **A91**, 644 (1967).

[16] S. Wynchank, H. Ceulemans, J. Garg, H. Liou, J. Rainwater, and W. W. Havens, Jr., Columbia University Progress Report, 1967, p. 1 (unpublished); and (private communication).

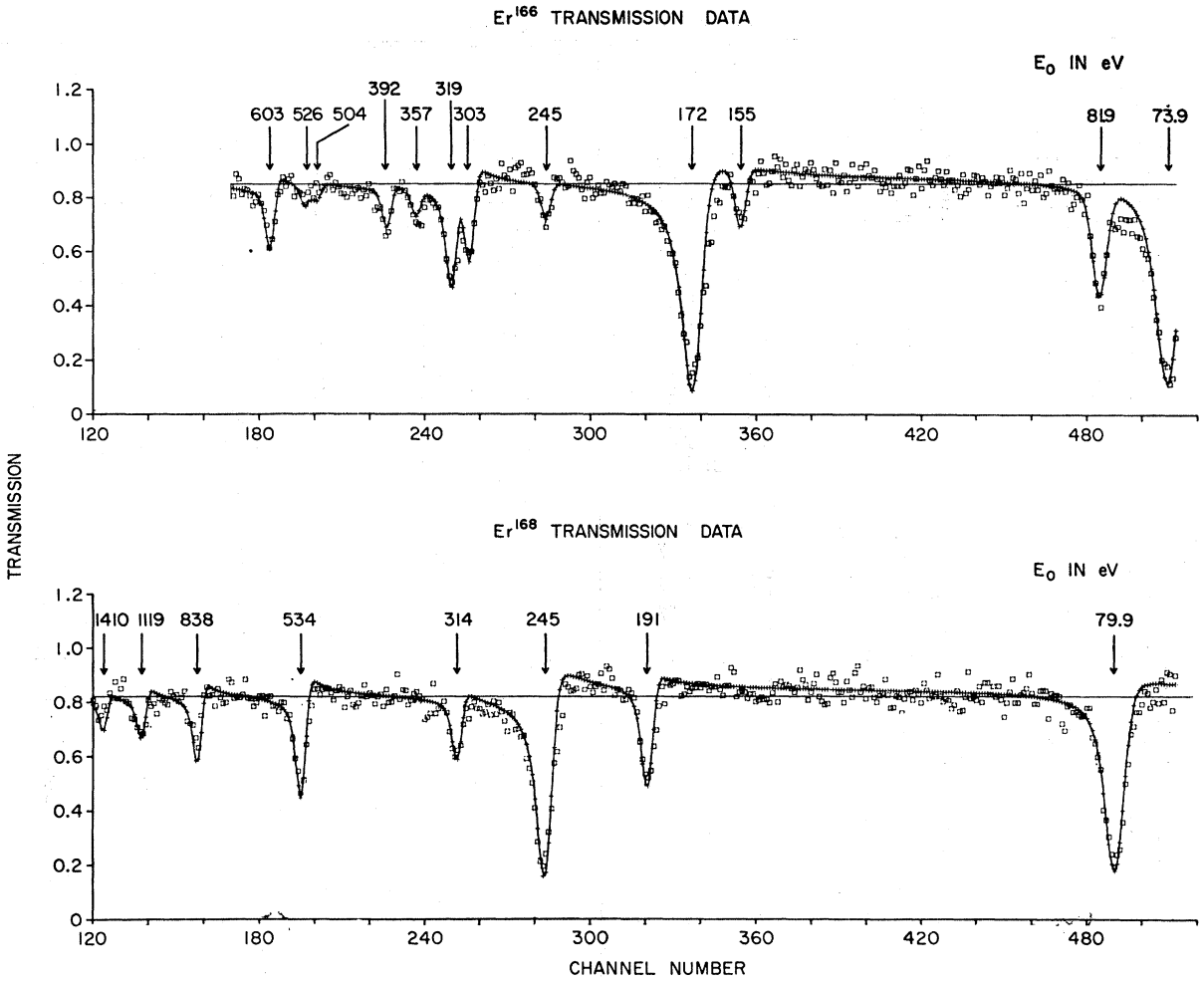

FIG. 4. The fitted transmission curves of Er^{166} and Er^{168} in the higher energy region. Er^{168} does not have any positive energy resonances below 79.9 eV.

Examples of the transmission curves of the higher energy runs are given in Fig. 4. Again we notice here that Er^{166} and Er^{168} have a common resonance at 245 eV. This resonance, appearing in the transmission of the Er^{166} sample, can not possibly be accounted for by an Er^{168} impurity. There are indications from our results that the 1410-eV level is actually two resonances. This is substantiated by the Columbia measurements.[16] The main deficiences in the curve fitting are to be found at the peaks and at the low-energy sides of the resonances. This effect has been studied carefully in Th^{232} and has been explained as largely being due to the presence of a tail in the resolution function.[14] The neutron widths are included in Table II. The error given for the resonance energies is derived from the full width of the resolution function at half-maximum. The errors on the neutron widths are obtained principally from statistics, uncertainty in determining the base line, and an uncertainty of 9 mV in the radiation width.

B. Potential Scattering Radius R'

The ability to fit the transmission data over a wide energy region containing many resonances enables one to extract a potential scattering radius R'. Most of the samples had a transmission of between 0.8 and 0.9 between resonances. Normalization errors are reduced to a minimum because of the unique cycling procedure which was described earlier. Such types of errors were estimated to be about 2% from the internal consistency between various runs. Since the samples are in oxide form, a correction due to oxygen scattering was applied. The most troublesome correction, however, is due to the small amount of water present in these oxide samples. This correction is negligible in resonance-parameter analysis, because it can be included in the base line, but it becomes significant when one desires to obtain R' from the data. For this reason it became necessary to study water absorption in the Er samples in a separate experiment, by taking a sample of natural

TABLE II. Resonance parameters.

E_0 (eV)	Γ_n (meV)	Γ_n^0 (meV)
	Er^{162}	
5.48 ± 0.08	0.32± 0.03	0.14 ± 0.01
7.60 ± 0.12	0.66± 0.05	0.24 ± 0.02
14.6 ± 0.1	4.1 ± 0.3	1.07 ± 0.08
20.3 ± 0.1	8.3 ± 0.8	1.84 ± 0.18
33.0 ± 0.2	5.0 ± 0.5	0.87 ± 0.09
43.2 ± 0.3	2.2 ± 0.2	0.33 ± 0.03
46.0 ± 0.3	19.5 ± 1.5	2.88 ± 0.22
51.4 ± 0.3	52 ± 6	7.25 ± 0.84
57.5 ± 0.4	32 ± 3	4.2 ± 0.4
67.8 ± 0.5	3.1 ± 0.5	0.38 ± 0.06
112.1 ± 1.1	12.7 ± 1.1	1.2 ± 0.1
127.0 ± 1.3	29.3 ± 5.6	2.6 ± 0.5
142.6 ± 1.6	14.3 ± 2.4	1.0 ± 0.2
158.5 ± 1.8	93 ± 25	7.4 ± 2.0
187.8 ± 2.3	41 ± 14	3.0 ± 1.0
210.2 ± 2.8	128 ± 37	8.8 ± 2.6
228.5 ± 3.2	54 ± 15	3.6 ± 1.0
	Er^{164}	
7.92 ± 0.02	0.73± 0.13	0.26 ± 0.05
30.5 ± 0.2	4.4 ± 0.4	0.80 ± 0.07
49.7 ± 0.4	5.4 ± 0.4	0.77 ± 0.06
53.8 ± 0.4	2.3 ± 0.2	0.31 ± 0.06
56.7 ± 0.4	6.6 ± 0.5	0.88 ± 0.07
108.1 ± 1.0	57 ± 6	5.2 ± 0.6
130.8 ± 1.4	104 ± 15	9.2 ± 1.3
136.5 ± 1.4	9.9 ± 2.2	0.86 ± 0.19
160.9 ± 1.9	61 ± 15	4.8 ± 1.2
194.2 ± 2.5	66 ± 8	4.9 ± 0.6
211.7 ± 2.9	31 ± 6	2.1 ± 0.4
225.2 ± 3.1	90 ± 15	6.0 ± 1.0
	Er^{166}	
15.56 ± 0.14	2.3 ± 0.2	0.58 ± 0.05
73.9 ± 0.6	60 ± 3	7.0 ± 0.3
81.9 ± 0.2	8.0 ± 0.8	0.88 ± 0.09
155 ± 2	7.0 ± 0.3	0.56 ± 0.02
172 ± 2	425 ± 20	32.4 ± 1.5
245 ± 4	21 ± 2	1.3 ± 0.1
303 ± 5	200 ± 15	11.5 ± 0.9
319 ± 5	318 ± 20	17.8 ± 1.1
357 ± 6	80 ± 15	4.3 ± 0.9
392 ± 7	155 ± 30	7.7 ± 1.5
504 ±11	31 ± 10	1.4 ± 0.4
526 ±11	90 ± 30	3.9 ± 1.3
603 ±14	570 ±100	23.2 ± 4.1
	Er^{167}	
0.460	0.31± 0.02	0.46 ± 0.04
0.584	0.24± 0.02	0.32 ± 0.03
5.98 ± 0.08	21 ± 3	8.6 ± 1.3
7.92 ± 0.12	0.22± 0.06	0.078± 0.021
9.35 ± 0.04	7.7 ± 0.4	2.5 ± 0.1
20.3 ± 0.1	5.2 ± 0.5	1.2 ± 0.1
22.0 ± 0.1	1.1 ± 0.1	0.23 ± 0.04
26.2 ± 0.1	105 ± 5	20.5 ± 1.0
27.5 ± 0.1	11.8 ± 3.1	2.25 ± 0.59
33.0 ± 0.2	6.2 ± 0.6	1.1 ± 0.1
37.7 ± 0.2	8.3 ± 0.7	1.4 ± 0.1
39.4 ± 0.2	7.5 ± 0.6	1.2 ± 0.1
42.4 ± 0.3	3.4 ± 0.3	0.52 ± 0.05
50.6 ± 0.3	7.4 ± 0.7	1.04 ± 0.10
53.8 ± 0.3	47 ± 5	6.4 ± 0.9
60.2 ± 0.4	16.1 ± 2.1	2.1 ± 0.3
62.9 ± 0.4	17.8 ± 2.2	2.2 ± 0.3
69.9 ± 0.6	2.4 ± 0.4	0.29 ± 0.05
74.1 ± 0.6	22 ± 2	2.5 ± 0.3
76.2 ± 0.6	0.5 ± 0.2	0.057± 0.023
79.4 ± 0.6	17.0 ± 1.4	1.91 ± 0.16
85.4 ± 0.7	0.91± 0.14	0.098± 0.015
91.5 ± 0.8	4.8 ± 0.6	0.50 ± 0.06
95.1 ± 0.8	25 ± 5	2.56 ± 0.51
107.9 ± 1.0	26 ± 4	2.5 ± 0.4
115.0 ± 1.2	2.5 ± 0.5	0.23 ± 0.05
131.8 ± 1.4	68 ± 10	5.9 ± 0.9
142.2 ± 1.6	14 ± 3	1.17 ± 0.25
	Er^{168}	
79.9 ± 0.7	39 ± 2	4.4 ± 0.2
191 ± 2	77 ± 7	5.6 ± 0.5
245 ± 4	535 ± 50	34.2 ± 3.2
314 ± 5	125 ± 20	7.1 ± 1.2
534 ± 6	845 ± 60	36.6 ± 2.6
838 ±23	1120 ±250	38.8 ± 8.7
1119 ±35	1120 ±400	33.5 ±11.9
1410 ±50	1100 ±450	29.3 ±12.0
	Er^{170}	
94.8 ± 0.8	902 ± 40	92.7 ± 4.2

erbium oxide and heating it in a platinum crucible for 2 h at 800°C under a vacuum of better than 10^{-5} mm Hg. Placing the samples in a desiccator after ignition proved to be ineffective in preventing water absorption. The increase in weight of the sample due to water absorption is found to be 0.26%. This correction factor was therefore applied to the data. The results are summarized in Table III and can be compared with the value 7.4 F, derived from $R=1.35\ A^{1/3}$ F.

C. *s*-Wave Neutron Strength Function

Two methods were adopted to obtain this quantity: (a) from the individual resonance parameters in the low-energy region, applying the relation

$$\text{strength function}=\frac{\langle g\Gamma_n^0\rangle}{D}=\Big(\sum_{i=1}^{N} g\Gamma_{n_i}^0\Big)/\Delta E, \quad (2)$$

where the summation is carried out on N resonances located in an energy interval $\Delta E=E_N-E_1$; and (b) from the slope of the average cross section in the unresolved energy region 5–15 keV. The two methods are illustrated in Figs. 5 and 6 for Er^{167}. In Fig. 5 the energy range is extended up to a neutron energy of 315 eV. Although individual resonances of Er^{167} are not well resolved above a neutron energy of 170 eV, the values obtained from the analysis above this energy can contribute a meaningful result to the strength function, and are included up to 315 eV. The aim behind this approach is to obtain a statistically significant result for this quantity. The results are included in Table III. The errors attached to the strength-function values when obtained from the parameters are derived from $(2/N)^{1/2}$, which is an asymptotic approximation derived from the Porter-Thomas distribution of reduced neutron widths. For Er^{167} in the neutron energy interval

TABLE III. Summary of results.

Isotope	R' (F)	$\frac{\langle g\Gamma_n^0\rangle}{D}\times 10^4$ (from resonances)	$\frac{\langle g\Gamma_n^0\rangle}{D}\times 10^4$ (from σ_{av})	$S^*\,10^4$	D (eV)	D^* (eV)
Er^{162}	8.1±0.9	2.1±0.7	2.1±0.6	$2.5^{+2.2}_{-1.0}$	6.9± 1.2	$6.8^{+1.6}_{-1.2}$
Er^{164}	9.2±0.8	1.6±0.5	1.4±0.3	$1.3^{+1.0}_{-0.5}$	20.0± 3.0	$21.2^{+4.4}_{-3.3}$
Er^{166}	7.7±0.9	1.9±0.7	···	$1.7^{+1.2}_{-0.7}$	49 ± 7	51^{+10}_{-8}
Er^{167}	9.9±0.9	2.6±0.4	1.7±0.2	$2.7^{+1.2}_{-0.7}$	3.7± 0.4	$3.9^{+0.5}_{-0.4}$
Er^{168}	6.6±0.8	1.4±0.7	···	$1.4^{+1.3}_{-0.6}$	125 ±19	126^{+27}_{-19}

170–315 eV, the number of levels have been estimated from a knowledge of D in the resolved energy region. Following the method of Muradyan and Adamchuk,[17] we have also evaluated the most probable value of the strength function, S^*, and its associated error, using the relation

$$S^*=Q^*\sum_{i=1}^{N}\Gamma_{ni}^0/(\pi\sum_{i=1}^{M}D_i^2)^{1/2}, \qquad (3)$$

where Q^* is determined from the maximum condition on the distribution of S. The summation is carried out on N resonances and M spacings. For the case where no resonances are missed, $M=N-1$. The calculations of S^* from the parameters are listed in Table III for the case of $M=N-1$. Inspecting Table III, one notices that the agreement between the two experimental methods of calculating the strength function in two different energy regions is generally quite good, except for Er^{167}, where the two values do not overlap within the experimental errors. If this difference is considered real, i.e., outside the statistical fluctuations it may be interpreted as being caused by a doorway state according to the Feshbach-Kerman-Lemmer model. It is significant to note that in this A region, fluctuations in the total cross section in the neutron energy range 100–600 keV have been recently observed[18] in the separated isotopes, W^{182}, W^{184}, and W^{186}.

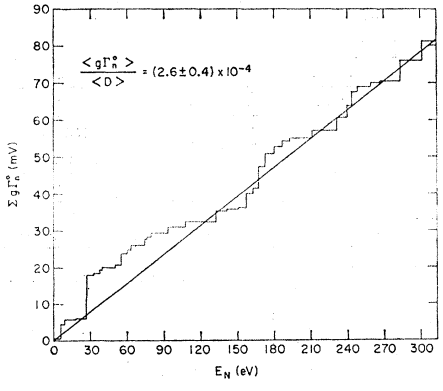

FIG. 5. The cumulative reduced neutron width for Er^{167} plotted against neutron energy up to an energy of 315 eV. The slope of the straight line is equal to the neutron strength function.

D. Spin Dependence of Level Densities

In what follows we shall base our calculations on the level-density formula derived on the basis of the Fermi-gas model.[19]

$$\rho(U,J)=\frac{C(2J+1)}{U^2}\exp\frac{-J(J+1)}{2\sigma^2}\exp 2(aU)^{1/2}, \qquad (4)$$

where J is the spin of the compound state, U is the

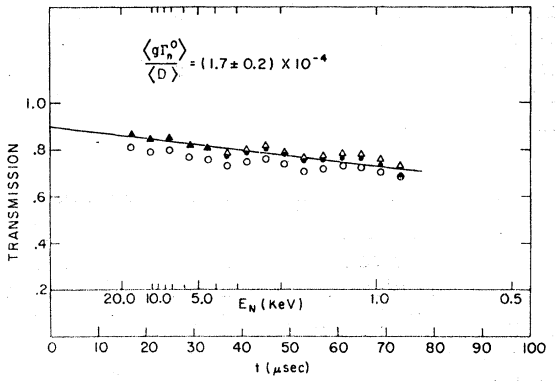

FIG. 6. The average transmission of Er^{167} in the keV region plotted against time-of-flight and energy. The meaning of the symbols are as follows: open circles indicate the experimental average transmission, triangles represent corrections for oxygen and isotopic impurities, closed circles represent corrections for sample thickness effects and level fluctuations of neutron reduced widths.

[17] H. V. Muradyan and Yu. V. Adamchuk, in *Nuclear Structure Study with Neutrons*, edited by M. Nève de Mévergnies *et al.* (North-Holland Publishing Company, Amsterdam, 1966), p. 569.

[18] A. B. Smith and J. F. Whalen, Bull. Am. Phys. Soc. **12**, 107 (1967); and (private communication).

[19] T. Ericson, Advan. Phys. **9**, 425 (1960).

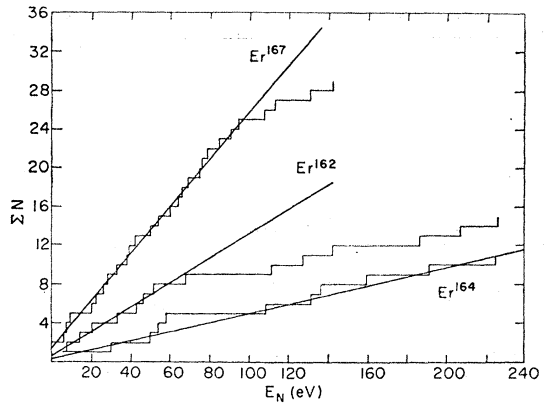

FIG. 7. The number of levels up to an energy E versus E for Er^{162}, Er^{164}, and Er^{167}. Note that above an energy of 67.5 eV for Er^{162}, small resonances are being missed mainly because of the masking effect of strong resonances of the isotopic impurities above this energy.

effective excitation energy defined below, a is the level density parameter, σ is the spin cutoff parameter, and C is a factor that depends on A. For slow neutrons, the effective excitation energy is expressed by

$$U=B_n-\Delta, \tag{5}$$

where B_n is the neutron binding energy, and for the compound nucleus,

$$\begin{aligned}\Delta&=\delta_n+\delta_p \text{ even-even},\\ &=\delta_p \text{ even-odd},\\ &=\delta_n \text{ odd-even},\\ &=0 \text{ odd-odd}.\end{aligned} \tag{6}$$

The neutron and proton pairing energies, δ_n and δ_p, have been taken from the work of Nemirovskii and Adamchuk.[20] It would be of particular interest to extract a value for σ from the observed average neutron level spacings. This factor is important in low-energy nuclear physics because it can be related to the nuclear temperature T and the moment of inertia I through the relation[19]

$$\sigma^2=TI/\hbar^2. \tag{7}$$

The average level spacings are obtained by the usual procedure described in Fig. 7 for Er^{162}, Er^{164}, and Er^{167}, where the integrated number of levels is plotted against energy. The results are listed in Table III. The error on D is given by $[(4-\pi)/\pi N]^{1/2}$, which is an asymptotic approximation derived from the Wigner distribution for level spacings. For comparison we have also included in the table the most probable values of the spacings, D^*, and the corresponding errors ΔD^*, calculated by the method of Muradyan and Adamchuk,[17] where

$$D^*=\left(\frac{\pi}{4M}\sum_{i=1}^{M}D_i^2\right)^{1/2}. \tag{8}$$

[20] P. E. Nemirovsky and Yu. V. Adamchuk, Nucl. Phys. **39**, 551 (1962).

The use of relation (4) to obtain σ requires a knowledge of a. Adopting a value of 19 MeV^{-1} for this parameter for the Er isotopes from Refs. 21 and 22, we obtain $\sigma=2.5\pm0.8$. This is in very good agreement with recent values derived from other types of nuclear data, such as (n,α),[23] $(n,2n)$,[23] and isomeric yield ratio measurements.[24] The implications of such a result is that the supposition of only a $(2J+1)$ dependence for level densities is not well obeyed for nuclei with high spin values. A similar conclusion had been reached by Hughes *et al.*,[25] from a study of fast neutron capture in various isotopes.

E. Thermal Cross Sections and Paramagnetic Scattering

It has been known for some time that the ions of the rare-earth elements have permanent magnetic moments caused by unfilled inner electron subshells. The influence of the magnetic moment on thermal neutrons is to give rise to a paramagnetic scattering. This would contribute an additional term to the total cross section

$$\sigma_T=\sigma_s+\sigma_{\rm pm}+\sigma_a, \tag{9}$$

where σ_s is the nuclear scattering, $\sigma_{\rm pm}$ is the paramagnetic scattering, and σ_a is the absorption cross section. The paramagnetic scattering can be written in the form[26]

$$\sigma_{\rm pm}=\tfrac{2}{3}\pi(e^2/mc^2)\gamma^2\mu^2\bar{F}^2, \tag{10}$$

where e^2/mc^2 is the classical electron radius, γ is the magnetic moment of the neutron, μ is the effective magnetic moment of the atom in Bohr magnetons, and F is the neutron scattering form factor. Equation (9) indicates that one can determine $\sigma_{\rm pm}$ if σ_T, σ_s, and σ_a are known. The measured total cross section of Er^{164} and Er^{168} at 0.0253 eV are 50 ± 8 b and 33.6 ± 2.0 b, respectively. Corrections have been made for dead-time count losses, water absorption by the samples, oxygen scattering, and isotopic impurities (for Er^{164}). The accuracy of these measurements is determined primarily by the uncertainty in the normalization, and to a lesser extent by counting statistics. The potential scattering cross sections for Er^{164} and Er^{168} are found to be 10.6 ± 1.8 and 5.5 ± 1.3 b, respectively. Using an absorption cross section[27] of 2.03 ± 0.41 b for Er^{168}, we

[21] E. Erba, U. Facchini, and E. Saetta Minichella, Nuovo Cimento **22**, 1237 (1961).
[22] J. A. Harvey, in *Neutron Time-of-Flight Methods*, edited by J. Spaepen (Euratom, Brussels, 1961).
[23] K. Breuer, B. Goel, K. N. Müller, and E. Rössle, in *Nuclear Structure Studies with Neutrons*, edited by M. Nève de Mévergnies *et al.* (North-Holland Publishing Company, Amsterdam, 1966), p. 542.
[24] P. Venugopala Rao and R. W. Fink, Phys. Rev. **154**, 1023 (1967).
[25] D. J. Hughes, R. C. Garth, and J. S. Levin, Phys. Rev. **91**, 1423 (1953).
[26] G. T. Trammel, Phys. Rev. **92**, 1387 (1953).
[27] R. F. Barnes, Argonne National Laboratory Report No. ANL 5287, 1954 (unpublished).

obtain $\sigma_{pm}=26.1\pm2.5$ b. This value is to be compared with a value of 23.5 b for the neighboring element Ho, obtained[28] from the experimental angular distribution of scattered neutrons, and a value of 27 b calculated by Zimmerman *et al.*[29] for natural erbium, using neutron scattering form factors calculated by Blume *et al.*[30] Finally, if we use $\sigma_{pm}=26.1\pm2.5$ b for Er^{164}, we get an absorption cross section for this isotope equal to 13 ± 9 b. Since the contribution of the positive energy resonances to the thermal absorption of Er^{164} is only 2 b, this indicates that Er^{164} has a bound level which contributes significantly to the thermal absorption cross section.

[28] T. E. Stephenson (private communication).
[29] R. L. Zimmerman, L. Q. Amaral, R. Fulfaro, M. C. Mattos, M. Abreu, and R. Stasiulevicius, Nucl. Phys. **A95**, 683 (1967).
[30] M. Blume, A. J. Freeman, and R. E. Watson, J. Chem. Phys. **37**, 1245 (1962).

ACKNOWLEDGMENTS

The authors gratefully acknowledge the assistance of I. W. Cole and J. Domish in performing calculations connected with this research.

PHYSICAL REVIEW VOLUME 162, NUMBER 4 20 OCTOBER 1967

One- and Three-Quasiparticle States of Odd-Mass Ni Isotopes*

Y. K. GAMBHIR AND RAM RAJ
Saha Institute of Nuclear Physics, Calcutta, India

AND

M. K. PAL†
Institute of Theoretical Science and Department of Physics, University of Oregon, Eugene, Oregon

(Received 29 May 1967)

The modified Tamm-Dancoff approximation has been used to study the states of odd-mass Ni isotopes as the superposition of one- and three-quasiparticle states. The three-quasiparticle basic states are classified according to the well-known seniority scheme and are expressed in an equivalent second-quantized form. These three-quasiparticle states form an orthonormal and nonredundant set. The effect of the spurious 0^+ two-quasiparticle state has also been removed from these basis wave functions. Several different kinds of two-body residual interaction have been used in the calculation. Fairly decent agreement is obtained in the energy spectra between our results and the exact shell-model results, using the effective interaction of Cohen *et al.* Various approximate methods, such as the perturbation theory and a phonon approximation, are discussed in the context of the present method. The effect of the ground-state correlation is also studied. The admixture of the three-quasiparticle states in the lowest few levels causes very little change in the magnetic moment, and the $M1$ transition rates calculated on the basis of a single-quasiparticle structure of these states. The $E2$ transition rate is fairly sensitive to the admixture and the type of interaction used.

1. INTRODUCTION

THE nuclear shell model has been successfully applied to the description of nuclei having few nucleons in the unfilled major shell. This line of approach becomes very complicated with the increase of number of nucleons due to the large number of near degenerate configurations involved. Such calculations are made possible by the development of the superconductivity (BCS) model[1,2] of the nucleus, which takes into account the strong "pairing interaction" between nucleons by the Bogoliubov-Valatin transformation resulting in quasiparticles. In the lowest approximation, the model interprets the first few low-lying states of odd-A nuclei as independent one-quasiparticle excitations. The first 2^+ state of spherical even nuclei, the so-called one-phonon state, is described as a superposition of quasiparticle pair states in the framework of Tamm-Dancoff approximation (TDA) and as a superposition of quasiparticle pair and quasihole pair states in the framework of random-phase approximation (RPA). A better approximation for odd-mass nuclei, then, is to mix the independent quasiparticle states with the states obtained by coupling single quasiparticles to this phonon state. Hereafter, this will be referred to as the phonon approximation (PA).

A more rigorous procedure is to do the configuration-mixing calculation of quasiparticle residual interaction in an enlarged space of all the one- and three-quasiparticle states. Such calculations involve technical difficulty in the construction of three-quasiparticle basic states when all the three-quasiparticles are in the same level.

* A preliminary report on this work has been published in the Proceedings of the Low Energy Nuclear Physics Symposium Kanpur, 1967 (unpublished) held by the Department of Atomic Energy, Government of India.
† Permanent address: Saha Institute of Nuclear Physics, Calcutta, India.
[1] L. S. Kisslinger and R. A. Sorensen, Kgl. Danske Videnskab. Selskab, Mat. Fys. Medd. **32**, No. 9 (1960).
[2] M. Baranger, Phys. Rev. **120**, 957 (1960).